Measurement of the phosphorite ore pulp density based on the image recognition method

Xianhai Li*, Han Li, Jiying Zhang, Fan Zhou and Aoao Chen

Mining College,
Guizhou University,
Guiyang 550025, China
and
National and Local Joint Laboratory of Engineering for Effective Utilization of Regional Mineral Resources from Karst Areas,
Guiyang 550025, China
and
Guizhou Key Lab of Comprehensive Utilization of Non-metallic Mineral Resources,
Guiyang 550025, China
Email: xhli1@gzu.edu.cn
Email: lihan668@163.com
Email: 342370875@qq.com
Email: kuangyuanzhoufan@163.com
Email: 18212106728@163.com
*Corresponding author

Abstract: In this paper, the image recognition method was applied to determine the phosphorite ore pulp density in the field of mineral processing engineering. The self-designed image recognition method-based ore pulp density measurement system was used to measure the density of phosphate ore pulp and conduct the feasibility analysis. The test results indicate that the grey value of phosphate ore pulp with different densities matched well with the pulp value. The test error of the ore pulp density of phosphate ore was 0.72%–1.23%, which could basically satisfy the requirements of industrial application with little discreteness, high accuracy and high precision. This study proves that it was feasible to measure phosphate ore pulp density by using an image recognition method and provides a new idea for ore pulp density measurement and some thoughts for the application of image recognition in mineral processing engineering.

Keywords: image recognition; phosphorite ore; characteristic colour; exponential approximation curve; ore pulp density.

Reference to this paper should be made as follows: Li, X., Li, H., Zhang, J., Zhou, F. and Chen, A. (2022) 'Measurement of the phosphorite ore pulp density based on the image recognition method', *Int. J. Mining and Mineral Engineering*, Vol. 13, No. 1, pp.64–75.

Biographical notes: Xianhai Li is currently a teacher at the Mining College of Guizhou University. He obtained his PhD from the College of Materials and Metallurgy, Guizhou University, Guiyang, China. His research field is focused on beneficiation of refractory ores and comprehensive utilisation of resources.

Han Li is an undergraduate of Mineral Processing Engineering in the College of Mining, Guizhou University. His research content of extra-curricular is the application of image recognition technology in mineral processing engineering.

Jiying Zhang is an undergraduate of Mineral Processing Engineering in the College of Mining, Guizhou University. His research content of extra-curricular is the application of image recognition technology in mineral processing engineering.

Fan Zhou is an undergraduate of Mineral Processing Engineering in the College of Mining, Guizhou University. His research content of extra-curricular is the application of image recognition technology in mineral processing engineering.

Aoao Chen is an undergraduate of Mineral Processing Engineering in the College of Mining, Guizhou University. His research content of extra-curricular is the application of image recognition technology in mineral processing engineering.

1 Introduction

Phosphate ore is an important non-metallic mineral resource for the fertiliser industry, and most phosphate resources are medium and low grade, which usually require processing to recover phosphate by rejecting gangue impurities prior to its application (Ye et al., 2018; Smith and You, 1995). In the process of phosphate ore beneficiation, ore pulp density is an essential production parameter to obtain high quality phosphorus concentrate. Ore pulp density is recognised as an essential production parameter and directly affects the technical and economic indices (Yu et al., 2015; Moghaddam et al., 2015; Hoang et al., 2019; Palencia et al., 2002; Yang et al., 2018; Gao et al., 2018; Tripathy and Murthy, 2012), such as the recovery rate, grade, reagent dosage, treatment capacity, and water consumption. The ore pulp density is defined as the content of solid ore particles in pulp, which is usually expressed by the liquid-solid ratio and solid mass percentage. At present, different types of density instruments have different working principles and can be classified into static pressure methods, gravity methods, float methods, gamma ray methods, vibration methods, photoelectric methods, ultrasonic methods, etc. The commonly used density measurement methods are direct measurement, density pot measurement, artificial experience and online density detection. Commonly used online density detectors include radioactive density metres, ultrasonic density metres and photoelectric density metres. Although the gamma ray density metre has high precision and a large range, it has potential safety hazards and gamma ray pollution. The ultrasonic density metre is not suitable for use in the case of low density and is greatly affected by bubbles; therefore, it cannot be used to measure the pulp density in the flotation cell. The photoelectric density metre has a small measuring range and is greatly affected by the chromaticity. The measuring tube of the vibration-type density metre is badly worn by pulp, and the instrument is more expensive. The pressure measurement used by the differential pressure density metre is easily affected by the impact of flow and not accurate in the case of low density. In actual mineral processing, density pots are

most widely used to measure ore pulp density because of the simple equipment to face the complex production environment and frequent fluctuation of production indices.

With the rapid development of computer science and image processing, increasing attention has been given to the research and application of image recognition, and many results have been achieved in many fields (Zhang et al., 2019; Li et al., 2013). Image recognition is a method to obtain image information and subsequently realise image recognition by using a computer to process, analyse and understand the expression of an image based on image shape characteristics, colour characteristics, texture characteristics, etc. with high accuracy, strong expressiveness and flexibility (Shuanhai et al., 2017; Köse et al., 2012; Iglesias et al., 2011; Donskoi et al., 2007). Image recognition technology can be understood as the initial digital image processing technology, which first appeared in the USA in 1960s (Andreopoulos and Tsotsos, 2013; Shuqiang et al., 2016), and computers were used to process image information from that time. Since the middle of the 1970s, with the rapid development of computer technology, digital image processing has developed to an increasingly deeper level. In recent years, the research and application of image recognition have increased in many fields, especially in biometric recognition and satellite clouds. Image recognition must go through the steps of pre-processing, region segmentation, characteristic extraction, etc. the algorithms of which are various and vary greatly among them with basically same general process. Image recognition technology has been widely applied in mechanics, surveying, architecture, material science, sociology and other fields (Li et al., 2016; Yanping et al., 2005; Xiaohui et al., 2011; Chengquan et al., 2013; Chun et al., 2018; Huang et al., 2018; Chunlin et al., 2008).

In the field of mining, image recognition technology is mainly used in geological exploration, ore particle size detection, flotation foam analysis, paste filling, mine gas alarm, recycling of waste resources, etc. (Kistner et al., 2013; Wang et al., 2019; Meshkani et al., 2013; Maitre et al., 2019; Hang et al., 2011; Hart et al., 2006; Habrat and Młynarczuk, 2018). Ghosh et al. (2013) successfully sorted alumina-rich iron ores according to the thermal image captured by IR thermography based on image recognition technology. Leroy et al. (2019) described an experimental setup designed for the multispectral imaging of particles in water suspensions to realise that images are processed to provide analysis on hundreds of particles in a few seconds. Aldrich (Fu and Aldrich, 2019) extracted the characteristics from froth images and used these characteristics as predictors to classify froth structures based on image recognition technology. Wang et al. (2018) studied a new system for image acquisition of lead flotation to monitor and optimise flotation production by image processing. Hao et al. (2019) introduced a method of bubble recognition using optical underwater images by employing Zernike moments and greyscale gradients to differentiate bubbles from solid particles. An extensive review of the literature shows that there may not be relevant research and applications of ore pulp density measurement based on image recognition technology at present in terms of ore pulp density measurement.

In this paper, according to the relevant principle of the image recognition method, a self-designed ore pulp density measurement system was designed. According to the correlation between pulp colour and ore pulp density, an image recognition method was adopted to extract the characteristic colours of ore pulp with different densities and obtain the corresponding greyscale value. Mathematical tools were used to establish the correlation mathematical model of the ore pulp density and greyscale value. The self-designed image recognition method-based pulp density measurement system was

used to test the density of a representative phosphate ore from a phosphate ore processing plant in Guizhou Province and analyse the feasibility and scientificity of the ideas of the ore pulp density measurement system based on image recognition technology.

2 Working principle and structure design of the ore pulp density measurement system

2.1 Working principle of the ore pulp density measurement system

Different cleavage planes of ore particles have different colours; therefore, there is a statistical likelihood that a certain density of ore pulp has a certain colour for a specific particle group size of a specific ore. It can be further speculated that there is a certain correlation between ore pulp density and pulp characteristic colour of a particular ore in a particular certain size composition. Based on the above analysis, the characteristic colour information of different densities of ore pulp can be extracted and quantified by image recognition technology. In this research, the greyscale value was used as colour information (Yue et al., 2018; Lipowezky, 2006; Horiuchi, 2006). A series of characteristic colour information (greyscale value) with a certain step length and the corresponding ore pulp density value were matched by an aexp(bx) + cexp(dx) exponential approximation curve to establish the mathematical model (called the standard curve in this paper). According to the function relation of the standard curve, the ore pulp density can be calculated and tested. The working principle of the ore pulp density measurement system based on image recognition technology is shown in Figure 1.

Figure 1 Schematic diagram of working principle of the ore pulp density measurement system (see online version for colours)

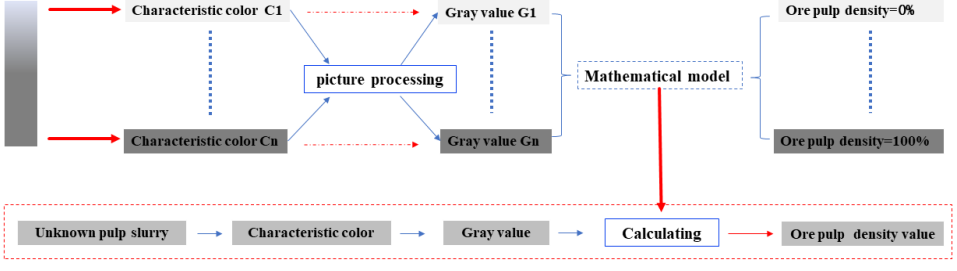

2.2 Structural design of the ore pulp density measurement system

According to the working principle of the ore pulp density measurement system in 2.1, the self-designed image recognition method-based ore pulp density measurement system was mainly composed of the measured ore pulp density measurement system and standard curve measurement system. The main components of the two systems were an image acquisition unit, a light supplement unit, a data processing unit and a data output unit, and the two systems were integrated into one system. The structure design of the ore pulp density measurement system is shown in Figure 2.

The image acquisition unit was mainly a camera, and the camera in this research was a complementary metal-oxide semiconductor (CMOS) camera and image acquisition software (MER-500-7UM-L). The characteristic image information of the measured ore pulp was converted into image data by the image acquisition unit. The light supplement unit was mainly composed of two white light LED lamps with controllable illumination, whose main function was to maintain a suitable light intensity in the image acquisition environment. The light intensity was certain to ensure that the incident light intensity of the test object was a fixed value for a specific test environment to validate the test data for each measurement. The data processing unit included the image data processing program, standard curve fitting program and density calculation program. The image data processing program calculated the greyscale value of each pixel in the image and obtained the average greyscale value of the image. The standard curve fitting program fit the greyscale value and corresponding ore pulp density value and established the standard curve. The density calculation program calculated the ore pulp density according to the standard curve using the calculated greyscale value. The main function of the data output unit was to output the calculated ore pulp density value and display it on the computer screen to conveniently measure the ore pulp density.

Figure 2 Structure design diagram of ore pulp density measurement system (see online version for colours)

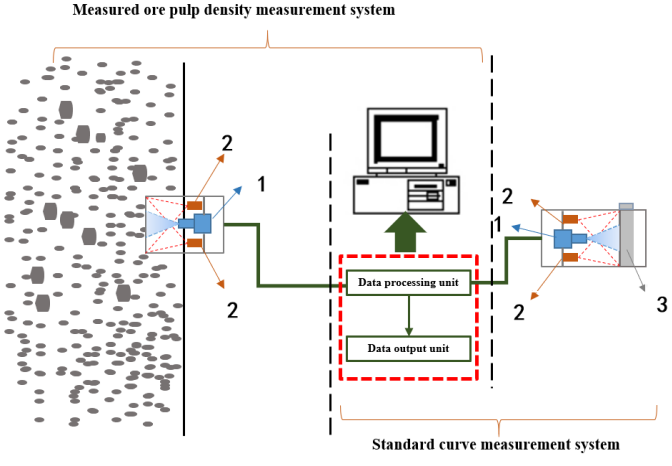

Note: 1 – image acquisition unit, 2 – light supplement unit and 3 – standard specimen cell.

3 Image recognition and data processing

The greyscale value $g(x, y)$ of a point in a two-dimensional image depends on the illuminance $i(x, y)$ of the corresponding point of the object in the space environment and the reflectivity $\gamma(x, y)$ of the point. The illuminance is determined by the light source, and the reflectivity is determined by the surface property of the object (Fanqin and Yaocai, 2003). For the specific size of the particle group of a specific ore, the surface property of the ore pulp is determined by the ore pulp density. Therefore, the greyscale value $g(x, y)$ of the two-dimensional image is a function of pulp density v to determine the

illuminance, and the expression formula of greyscale value $g(x, y, v)$ is shown in formula (1):

$$g(x, y, v) = i(x, y)\gamma(x, y, v) \tag{1}$$

In the single-channel greyscale image, the greyscale value reflects the degree of white of pixel point (i, j), which is 0–255 (white is 255, and black is 0). The characteristic colour of every image from a digital camera is composed of numerous ordered pixels with a specific greyscale (see Figure 3). As shown in Figure 3, a two-dimensional image collected is a matrix integrated by countless pixel points (i, j), and every pixel point has a corresponding specific greyscale value. Assuming that the ore particles are sufficiently dispersed and uniform in the ore pulp and the granularity level of the particle group is sufficiently narrow, the greyscale value of every pixel in every ore pulp image is a fixed value. However, it is difficult to realise this ideal state in the specific operation process, and it is necessary to process the collected image. The ore pulp density measurement system based on the image recognition method adopted the mean processing method for the greyscale value of pixel points in an image in this research, and the detailed operation procedure was as follows: first, the greyscale value of every pixel in the entire image was counted to obtain the number of pixel points corresponding to every greyscale value, and the number was represented by μ, such as μ_1, μ_2, μ_3, μ_4, ⋯, μ_{255}. Second, the greyscale values of all pixel points in an image were averaged to obtain the characteristic greyscale value of this image, as shown in formula (2).

$$g(i) = \frac{1}{\sum_{i=0}^{255} \mu i} \sum_{i=0}^{255} (i \cdot \mu i) \tag{2}$$

$$F(a, b, c, d) = \sum_{i=0}^{m} (vi - v(gi))^2 \tag{3}$$

$$v(gi) = a \cdot \exp(b \cdot gi) + c \cdot \exp(d \cdot gi) \tag{4}$$

Figure 3 An example of two-dimensional greyscale image (see online version for colours)

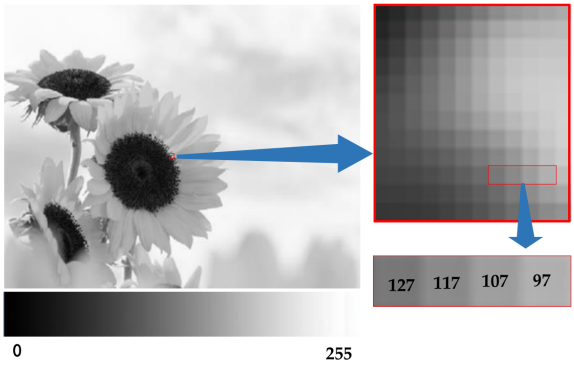

The image recognition method could realise the extraction of characteristic information of ore pulp images with a certain density. It was necessary to establish a mathematical model of the greyscale value and corresponding ore pulp density value to determine the ore pulp density by image recognition. The basic idea was as follows: collected and

processed images of a series of ore pulp with a known density with a certain step length to obtain a series of image characteristic greyscale values and established the data group (gi, vi) (i = 0, 1, 2, 3, ⋯, m). The functional relationship between greyscale value and ore pulp density from the data group (gi, vi) was matched by an aexp(bx) + cexp(dx) exponential approximation curve to establish the standard curve (Chen et al., 2011; Yuechao et al., 2011), to achieve the maximum approximation of the standard curve to all data in the data group (gi, vi). To realise this basic idea, the nonlinear fitting problem was transformed into a linear fitting problem; then, the nonlinear fitting function was obtained through inverse transformation. According to the principle of least squares, the appropriate a, b, c and d values were selected to minimise $F(a, b, c, d)$ in formula (3).

4 Ore pulp density testing and feasibility analysis

It is known that different ores have different physical and chemical properties and different optical properties. In this research, a typical silica-calcareous phosphate ore from a phosphate ore processing plant in Guizhou Province was selected as a test specimen to measure the pulp density using a self-designed image recognition method-based ore pulp density measurement system to test the feasibility and scientificity of the ideas.

4.1 Establishment of a standard curve

The phosphate ore was ground to a particle size of –0.075 mm, accounting for 80%, and the particle size distribution of ore after grinding is shown in Table 1. Ore pulp was accurately prepared with densities of 50.00% and 60.00% because the effective separation ranges of phosphate ores is generally no less than 10.00% and no more than 60.00%. The characteristic images of different ore pulp densities collected by the self-designed image recognition method-based ore pulp density measurement system are shown in Figure 4. The image information in Figure 4 was converted into image data by image recognition technology, and the image data were calculated according to formula (2) to obtain the greyscale value of every image, which is shown in Table 2. The data in Table 2 were matched by formula (4) to establish the standard curve $v(gi) = (5.259 \times (10)^7) \times \exp(-0.09117 \times gi)$ and draw the standard curve (see Figure 5). The colour became darker, and the greyscale value gradually increased with increasing ore pulp density. The relevant fitting parameters of the standard curves are shown in Table 3. SSE is the sum-of-squares error, R-square is the coefficient of determination, adjusted R-square is the coefficient of determination after correction, and RMSE is the root mean squared error. Figure 5 and Table 3 show that the regularity is obvious for the curves, which is consistent with the exponential approximation curve with a high fitting degree and applicability.

Table 1 Particle size distribution of ore in pulp

Particle size/mm	*+0.15*	*–0.15 + 0.09*	*–0.09 + 0.075*	*–0.075 + 0.045*	*–0.045*
Content/%	1.02	6.21	13.12	30.03	49.62

Table 2 Correlation data table of ore pulp density and average greyscale value.

Parameter	*Ore pulp density /%*					
	10.00	*20.00*	*30.00*	*40.00*	*50.00*	*60.00*
Averages greyscale value	169.4780	162.0140	157.6629	153.9738	151.8979	150.5687

Figure 4 Characteristic images of phosphate ore pulp with different densities

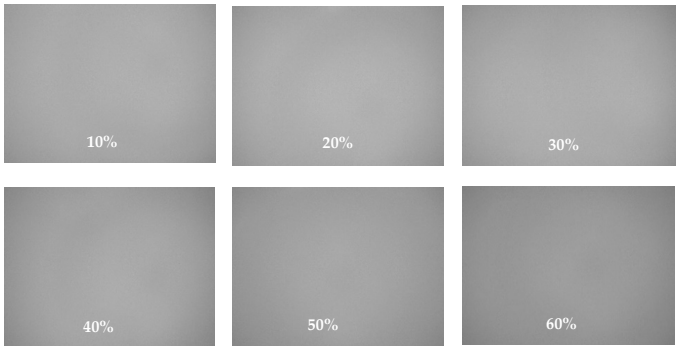

Figure 5 Standard curve of phosphate ore matched by the aexp(bx) + cexp(dx) exponential approximation curve (see online version for colours)

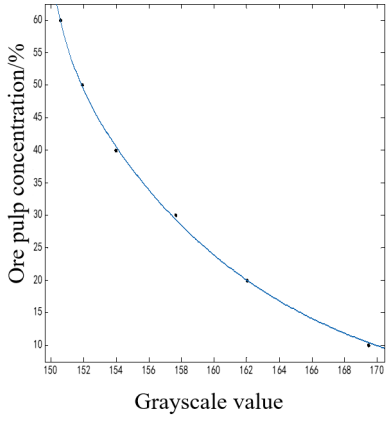

Table 3 Standard curve fitting parameters for ore pulp density testing.

Specimen	*SSE*	*R-square*	*Adjusted R-square*	*RMSE*
Phosphate ore	1.052	0.999	0.999	0.725

4.2 Measurement of ore pulp density

Every measured specimen with different densities (14.00%, 25.00%, 32.00%, 38.00% and 42.00%) was tested ten times and calculated based on the standard curves in 4.1 as shown in Table 4. The mean value of the 10 times testing data was defined as the measured value (MV), and DV is the determined value of ore pulp density. MD is the

difference between the measured value and determined value (MD = MV – DV). The confidence interval of each group of data was calculated to reflect the reliability of the method for ore pulp testing as shown in Table 5. To minimise human error, the test method has high accuracy in measuring pulp concentration, especially for the pulp concentration of 25–32. As a whole, the difference between measured value and determined value was relatively low, and the test error of the ore pulp density and phosphate ore did not exceed 1.23%.

Table 4 Comparison of the measured and true values of ore pulp density of phosphate ore

Specimen series	*Ore pulp density (DV)/%*	*Measured value 1/%*	*Measured value 2/%*	*Measured value 3/%*	*Measured value 4/%*	*Measured value 5/%*	*Measured value 6/%*
No. 1	14.00	15.11	14.95	15.03	14.43	13.95	15.21
No. 2	25.00	26.25	26.08	25.79	25.35	25.67	25.83
No. 3	32.00	31.44	30.54	31.86	31.12	31.09	31.54
No. 4	38.00	36.52	36.21	36.78	35.67	35.84	37.76
No. 5	42.00	40.91	40.31	42.65	41.43	40.65	40.89

Specimen series	*Measured value 7/%*	*Measured value 8/%*	*Measured value 9/%*	*Measured value 10/%*	*Mean value (MV)/%*	*MD/%*
No. 1	14.89	13.98	15.35	16.07	14.90	–0.90
No. 2	25.32	26.75	25.42	25.88	25.83	–0.83
No. 3	31.03	31.68	31.67	30.85	31.28	0.72
No. 4	37.54	36.68	37.01	37.93	36.79	1.21
No. 5	41.22	39.61	39.85	40.22	40.77	1.23

Table 5 Results of confidence intervals

Specimen series	*No. 1*	*No. 2*	*No. 3*	*No. 4*	*No. 5*
Standard values	14.00	25.00	32.00	38.00	42.00
Sample mean	14.90	25.83	31.28	36.79	40.77
Sample std. dev.	0.64	0.44	0.42	0.78	0.88
Margin of error (95%)	0.46	0.32	0.30	0.56	0.63
Lower limit	14.44	25.52	30.98	36.24	40.15
Upper limit	15.36	26.15	31.58	37.35	41.40
Confidence intervals	[14.44, 15.36]	[25.52, 26.15]	[30.98, 31.58]	[36.24, 37.35]	[40.15, 41.40]

5 Conclusions

The image recognition method was applied to measure the ore pulp density in mineral processing engineering. After conducting design, testing and feasibility analysis of the ore pulp density measurement system based on the image recognition method, we obtain the following conclusions:

1 There is a certain correlation between ore pulp density and pulp characteristic colour of a particular ore in a particular certain size composition. The image recognition method was adopted to extract the characteristic colours of ore pulp with different densities and obtain the corresponding greyscale value. The functional relationship between greyscale value and ore pulp density from the data group (gi, vi) (i = 0, 1, 2, 3, ⋯, m) was matched by an aexp(bx) + cexp(dx) exponential approximation curve to establish the standard curve. The standard curve and density measurement were conducted by using the self-designed image recognition method-based ore pulp density measurement system. The experimental results proved that it was feasible to measure the ore pulp density by using the image recognition method and provided a new method for ore pulp density measurement.

2 The self-designed image recognition method-based ore pulp density measurement system was mainly composed of the measured ore pulp density measurement system and the standard curve measurement system. The main components of the two systems were an image acquisition unit, a light supplement unit, a data processing unit and a data output unit. The two systems were integrated into one system, and all units were controlled by a computer.

3 The self-designed image recognition method-based ore pulp density measurement system was used to test the ore pulp density of phosphate ore. The test results of phosphate ore were of high accuracy and precision. The test error of the ore pulp density of phosphate ore did not exceed 1.23%.

Acknowledgements

This work was financially supported by the National Key R&D Program of China, 2018YFC1903500 and the Guizhou University High-level Talent Scientific Research Project (GZU R.J.H. 202177).

References

Andreopoulos, A. and Tsotsos, J.K. (2013) '50 years of object recognition: directions forward', *Computer Vision and Image Understanding*, Vol. 117, No. 8, pp.827–891.

Chen, X., Wei, W., Liu, M. and Gu, G. (2011) 'Variations of snow temperature and their influence on snow cover physical parameters in the Western Tianshan Mountains, China', *Journal of Mountain Science*, Vol. 8, No. 6, pp.827–837.

Chengquan, D., Shengcai, Y., Hui, C. and Juntao, M. (2013) 'Study on application of image recognition technology to pile quality testing', *Chinese Journal of Engineering Geophysics*, Vol. 10, No. 5, pp.736–739.

Chun, L., Qiang, X., Bin, S. and Yingfan, G. (2018) 'Digital image recognition method of rock particle and pore system and its application', *Chinese Journal of Geotechnical Engineering*, Vol. 40, No. 5, pp.925–931.

Chunlin, Z., Hehua, Z. and Xiaojun, L. (2008) 'Application of infrared photography and image processing to tunnel construction with new Austrian tunneling method', *Chinese Journal of Rock Mechanics and Engineering*, Vol. 27, No. S1, pp.3166-3172.

Donskoi, E., Suthers, S.P., Fradd, S.B., Young, J.M., Campbell, J.J., Raynlyn, T.D. and Clout, J.M.F. (2007) 'Utilization of optical image analysis and automatic texture classification for iron ore particle characterisation', *Minerals Engineering*, Vol. 20, No. 5, pp.461–471.

Fanqin, M. and Yaocai, W. (2003) 'Study of the methods for recognizing the coal flow image of coal mine's conveyer belt', *Journal of China Coal Society*, Vol. 28, No. 1, pp.91–95.

Fu, Y. and Aldrich, C. (2019) 'Flotation froth image recognition with convolutional neural networks', *Minerals Engineering*, Vol. 132, pp.183–190.

Gao, Y., Zhang, G., Wang, M. and Liu, D. (2018) 'The critical role of pulp density on flotation separation of nickel-copper sulfide from fine serpentine', *Minerals*, Vol. 8, No. 8, p.317.

Ghosh, A., Nayak, B., Das, T.K. and Palit Sagar, S. (2013) 'A non-invasive technique for sorting of alumina-rich iron ores', *Minerals Engineering*, Vol. 45, pp.55–58.

Habrat, M. and Młynarczuk, M. (2018) 'Evaluation of local matching methods in image analysis for mineral grain tracking in microscope images of rock sections', *Minerals*, Vol. 8, No. 5, p.182.

Hang, S., Mercuri, P., Díaz-Zorita, M., Havrylenko, S. and Barriuso, E. (2011) 'Satellite images as a tool to identify accelerated atrazine mineralization in soils', *Crop Protection*, Vol. 30, No. 6, pp.663–670.

Hao, Z., Xiangchun, L., Qian, Y., Chenxuan, W. and Zhuo, L. (2019) 'Optical image recognition of underwater bubbles', *Infrared and Laser Engineering*, Vol. 48, No. 3, pp.270–276.

Hart, B., Biesinger, M. and Smart, R.S.C. (2006) 'Improved statistical methods applied to surface chemistry in minerals flotation', *Minerals Engineering*, Vol. 19, No. 6, pp.790–798.

Hoang, D.H., Hassanzadeh, A., Peuker, U.A. and Rudolph, M. (2019) 'Impact of flotation hydrodynamics on the optimization of fine-grained carbonaceous sedimentary apatite ore beneficiation', *Powder Technology*, Vol. 345, pp.223–233.

Horiuchi, T. (2006) 'Grayscale image segmentation using color space (image recognition, computer vision)', *IEICE Transactions on Information and Systems*, Vol. 89, No. 3, pp.1231–1237.

Huang, H., Li, Q. and Zhang, D. (2018) 'Deep learning based image recognition for crack and leakage defects of metro shield tunnel', *Tunnelling and Underground Space Technology*, Vol. 77, pp.166–176.

Iglesias, J.C.A., Gomes, O.D.F.M. and Paciornik, S. (2011) 'Automatic recognition of hematite grains under polarized reflected light microscopy through image analysis', *Minerals Engineering*, Vol. 24, No. 12, pp.1264–1270.

Kistner, M., Jemwa, G.T. and Aldrich, C. (2013) 'Monitoring of mineral processing systems by using textural image analysis', *Minerals Engineering*, Vol. 52, No. S1, pp.169–177.

Köse, C., Alp, O. and Ikibaş, C. (2012) 'Statistical methods for segmentation and quantification of minerals in ore microscopy', *Minerals Engineering*, Vol. 30, pp.19–32.

Leroy, S. and Pirard, E. (2019) 'Mineral recognition of single particles in ore slurry samples by means of multispectral image processing', *Minerals Engineering*, Vol. 132, pp.228–237.

Li, C.H., Zhang, J.B., Hu, X.P. and Zhao, G.F. (2013) 'Algorithm research of two-dimensional size measurement on parts based on machine vision', *Advanced Materials Research*, Vols. 694–697, pp.1945–1948.

Li, F., Luo, S., Liu, X. and Zou, B. (2016) 'Bag-of-visual-words model for artificial pornographic images recognition', *Journal of Central South University*, Vol. 23, No. 6, pp.1383–1389.

Lipowezky, U. (2006) 'Grayscale aerial and space image colorization using texture classification', *Pattern Recognition Letters*, Vol. 27, No. 4, pp.275–286.

Maitre, J., Bouchard, K. and Bédard, L.P. (2019) 'Mineral grains recognition using computer vision and machine learning', *Computers and Geosciences*, Vol. 130, pp.84–93.

Meshkani, S.A., Mehrabi, B., Yaghubpur, A. and Sadeghi, M. (2013) 'Recognition of the regional lineaments of Iran: using geospatial data and their implications for exploration of metallic ore deposits', *Ore Geology Reviews*, Vol. 55, pp.48–63.

Moghaddam, M.Y., Shafaei, S.Z., Noaparast, M., Ardejani, F.D., Abdollahi, H., Ranjbar, M., Schaffie, M. and Manafi, Z. (2015) 'Empirical model for bio-extraction of copper from low grade ore using response surface methodology', *Transactions of Nonferrous Metals Society of China*, Vol. 25, No. 12, pp.4126–4143.

Palencia, I., Romero, R., Mazuelos, A. and Carranza, F. (2002) 'Treatment of secondary copper sulphides (chalcocite and covellite) by the BRISA process', *Hydrometallurgy*, Vol. 66, No. 1, pp.85–93.

Shuanhai, H., Xiangmo, Z., Jian, M., Yi, Z., Huansheng, S., Hongxun, S., Lei, C., Zhuoya, Y., Fuwei, H., Jian, Z., Bin, T., Luyang, W. and Xiuzhen, Q. (2017) 'Review of highway bridge inspection and condition assessment', *China Journal of Highway and Transport*, Vol. 30, No. 11, pp.63–80.

Shuqiang, J., Weiqing, M. and Shuhui, W. (2016) 'Survey and prospect of intelligent interaction-oriented image recognition techniques', *Journal of Computer Research and Development*, Vol. 53, No. 1, pp.113–122.

Smith, M.L. and You, T.W. (1995) 'Mine production scheduling for optimization of plant recovery in surface phosphate operations', *International Journal of Surface Mining and Reclamation*, Vol. 9, No. 2, pp.41–46.

Tripathy, S.K. and Murthy, Y.R. (2012) 'Multiobjective optimisation of spiral concentrator for separation of ultrafine chromite', *International Journal of Mining and Mineral Engineering*, Vol. 4, No. 2, pp.151–162.

Wang, W., Liu, W., Lang, F., Zhang, G., Gao, T., Cao, T., Wang, F. and Liu, S. (2018) 'Froth Image acquisition and enhancement on optical correction and retinex compensation', *Minerals*, Vol. 8, No. 3, p.103.

Wang, Z., Peng, B., Huang, Y. and Sun, G. (2019) 'Classification for plastic bottles recycling based on image recognition', *Waste Management*, Vol. 88, pp.170–181.

Xiaohui, F., Zhonghua, Z., Xuling, C., Min, G. and Yi, W. (2011) 'Micrograph recogniziation and system development of sinter mineralogy', *Journal of Central South University (Science and Technology)*, Vol. 42, No. 10, pp.2893–2897.

Yang, C., Li, S., Zhang, C., Bai, J. and Guo, Z. (2018) 'Application of superconducting high gradient magnetic separation technology on silica extraction from iron ore beneficiation tailings', *Mineral Processing and Extractive Metallurgy Review*, Vol. 39, No. 1, pp.44–49.

Yanping, Q., Yanli, J., Weiqi, Y. and Xin, G. (2005) 'Application of image recognition technology in evaluating the color of material corrosion image', *Surface Technology*, No. 4, pp.71–72+75.

Ye, J., Wang, X., Li, X., Mao, S., Shen, Z. and Zhang, Q. (2018) 'Effect of dispersants on dispersion stability of collophane and quartz fines in aqueous suspensions', *Journal of Dispersion Science and Technology*, Vol. 39, No. 11, pp.1655–1663.

Yu, R., Wu, F., Chen, A., Shi, L., Zeng, W., Gu, G., Qin, W. and Qiu, G. (2015) 'Effect of mixed moderately thermophilic adaptation on leachability and mechanism of high arsenic gold concentrate in an airlift bioreactor', *Journal of Central South University*, Vol. 22, No. 1, pp.66–73.

Yue, Z., Qiaoling, H. and Yandong, Z. (2018) 'Improved FCM method for pore identification based on grayscale-gradient features', *Transactions of the Chinese Society of Agricultural Machinery*, Vol. 49, No. 3, pp.279–286.

Yuechao, S., Shuoshi, M., Zhi, C., Yonglai, Z. and Hongmei, C. (2011) 'Drought farmland near surface blown sand and wind erosion controlling effect', *Journal of Agricultural Machinery*, Vol. 42, No. 1, pp.54–58.

Zhang, L., Yang, Q., Sun, Q., Feng, D. and Zhao, Y. (2019) 'Research on the size of mechanical parts based on image recognition', *Journal of Visual Communication and Image Representation*, Vol. 59, pp.425–432.